

## OPEN

# Diagnostic Accuracy of Diffusion-Weighted Magnetic Resonance Imaging Versus Positron Emission Tomography/Computed Tomography for Early Response Assessment of Liver Metastases to Y90-Radioembolization

Alexandra Barabasch, MD,\* Nils A. Kraemer, MD,\* Alexander Ciritsis, Dipl-Ing,\* Nienke L. Hansen, MD,\* Marco Lierfeld, Dipl-Ing,\* Alexander Heinzl, MD,† Christian Trautwein, MD,‡ Ulf Neumann, MD,§ and Christiane K. Kuhl, MD\*

**Objectives:** Patients with hepatic metastases who are candidates for Y90-radioembolization (Y90-RE) usually have advanced tumor stages with involvement of both liver lobes. Per current guidelines, these patients have usually undergone several cycles of potentially hepatotoxic systemic chemotherapy before Y90-RE is at all considered, requiring split (lobar) treatment sessions to reduce hepatic toxicity. Assessing response to Y90-RE early, that is, already after the first lobar session, would be helpful to avoid an ineffective and potentially hepatotoxic second lobar treatment. We investigated the accuracy with which diffusion-weighted magnetic resonance imaging (DWI-MRI) and positron emission tomography/computed tomography (PET/CT) can provide this information.

**Methods:** An institutional review board–approved prospective intraindividual comparison trial on 35 patients who underwent fluorodeoxyglucose PET/CT and DWI-MRI within 6 weeks before and 6 weeks after Y90-RE to treat secondary-progressive liver metastases from solid cancers (20 colorectal, 13 breast, 2 other) was performed. An increase of minimal apparent diffusion coefficient (ADC<sub>min</sub>) or decrease of maximum standard uptake value (SUV<sub>max</sub>) by at least 30% was regarded as positive response. Long-term clinical and imaging follow-up was used to distinguish true- from false-response classifications.

**Results:** On the basis of long-term follow-up, 23 (66%) of 35 patients responded to the Y90 treatment. No significant changes of metastases size or contrast enhancement were observable on pretreatment versus posttreatment CT or magnetic resonance images. However, overall SUV<sub>max</sub> decreased from  $8.0 \pm 3.9$  to  $5.5 \pm 2.2$  ( $P < 0.0001$ ), and ADC<sub>min</sub> increased from  $0.53 \pm 0.13 \times 10^{-3} \text{ mm}^2/\text{s}$  to  $0.77 \pm 0.26 \times 10^{-3} \text{ mm}^2/\text{s}$  ( $P < 0.0001$ ). Pretherapeutic versus posttherapeutic changes of ADC<sub>min</sub> and SUV<sub>max</sub> correlated moderately ( $r = -0.53$ ). In 4 of the 35 patients (11%), metastases were fluorodeoxyglucose-negative such that no response assessment was possible by PET. In 25 (71%) of the 35 patients, response classification by PET and DWI-MRI was concordant; in 6 (17%) of the 35, it was discordant. In 5 of the 6 patients with discordant classifications, follow-up confirmed diagnoses made by DWI. The positive predictive value to predict response was 22 (96%) of 23 for MRI and 15 (88%) of 17 for PET. The negative predictive value to predict absence was 11 (92%) of 12 for MRI and 10 (56%) of 18 for PET. Sensitivity for detecting response was significantly higher for MRI (96%; 22/23) than for PET (65%; 15/23) ( $P < 0.02$ ).

**Conclusions:** Diffusion-weighted magnetic resonance imaging appears superior to PET/CT for early response assessment in patients with hepatic metastases of

common solid tumors. It may be used in between lobar treatment sessions to guide further management of patients who undergo Y90-RE for hepatic metastases.

**Key Words:** liver metastases, liver MRI, PET/CT, SUV, DWI, ADC, response assessment, Y90, radioembolization

(*Invest Radiol* 2015;50: 409–415)

**R**adioembolization (Y90-RE) is an established method for local treatment of otherwise therapy-refractory primary liver cancer and liver metastases of extrahepatic tumors.<sup>1,2</sup> Assessing response to local therapy, such as Y90-RE, is challenging. Determining tumor size as, for example, prescribed by Response Evaluation Criteria in Solid Tumors (RECIST) can be misleading owing to therapy-induced tissue transformation into necrosis or fibrosis.<sup>2–6</sup>

Therefore, functional imaging has been proposed to improve the accuracy with which response to local treatment can be determined. The uptake of fluorodeoxyglucose (FDG) quantified via standardized uptake value (SUV) on positron emission tomography/computed tomography (PET/CT) scans has been shown to be useful for the assessment of response to local treatment, including Y90-RE. The degree of therapy-induced SUV changes is an established parameter to predict tumor response to treatment and has also been shown to provide prognostic information because it correlates with overall survival after RE.<sup>5–7</sup>

Diffusion-weighted magnetic resonance imaging (DWI-MRI) has been shown to provide diagnostic information that can be used to demonstrate treatment effects similar to PET.<sup>8–10</sup> It has been shown that the DWI-derived apparent diffusion coefficient (ADC) of primary cancers and liver metastases increases after neoadjuvant chemotherapy<sup>11,12</sup> and that these ADC changes correlate with PET-derived SUV changes.<sup>13–20</sup> However, there is only anecdotal evidence available on the use of DWI for response assessment in metastases of solid tumors to local<sup>21,22</sup> or systemic treatment.<sup>11</sup> Hence, although DWI has been in clinical use for a decade already<sup>10</sup> and has been proposed for functional response assessment since then, the diagnostic accuracy with which DWI-MRI can detect early response to treatment has, so far, not been established. Moreover, it is unclear how the diagnostic accuracy of DWI with regard to early response assessment compares with the diagnostic accuracy afforded by PET.

Therefore, we set out to intraindividually compare response assessment on the basis of DWI versus PET/CT in patients with liver metastases who underwent Y90-RE and who underwent systematic clinical and imaging follow-up to validate the respective imaging diagnoses suggested by both DWI and PET/CT for response assessment.

## PATIENTS AND METHODS

This institutional review board–approved prospective intraindividual diagnostic trial was conducted at an academic comprehensive cancer center. Written informed consent was obtained from all participants.

Received for publication September 9, 2014; and accepted for publication, after revision, January 14, 2015.

From the Departments of \*Diagnostic and Interventional Radiology, †Nuclear Medicine, ‡Internal Medicine III, and §General, Visceral and Transplantation Surgery, University Hospital RWTH Aachen, Aachen, Germany.

Conflicts of interest and sources of funding: none declared.

Reprints: Christiane K. Kuhl, MD, Department of Diagnostic and Interventional Radiology, University Hospital RWTH Aachen, Pauwelsstr. 30, 52074 Aachen, Germany. E-mail: ckuhl@ukaachen.de.

Copyright © 2015 Wolters Kluwer Health, Inc. All rights reserved. This is an open access article distributed under the terms of the Creative Commons Attribution-NonCommercial-NoDerivatives 3.0 License, where it is permissible to download and share the work provided it is properly cited. The work cannot be changed in any way or used commercially.

ISSN: 0020-9996/15/5006–0409

## Patient Cohort

Patients meeting the following criteria were included: lobar RE performed for unresectable metastatic liver disease with at least 3 recognizable liver metastases of at least 1 cm in size, secondary progressive after appropriate systemic treatment, without prior intra-arterial therapies. To avoid repeat observations made in the same patient, every patient was included only once, although most patients underwent 2 (or more) lobar or segmental RE sessions.

## Y90 Radioembolization

The decision to perform RE was made for each patient case in a dedicated gastrointestinal multidisciplinary tumor conference. The patients had progressive hepatic tumor load despite having undergone appropriate systemic chemotherapy according to guidelines established for the respective tumor entity; liver metastases were considered prognostically dominant, and the patients had a normal liver function and Eastern Cooperative Oncology Group-0/1 status. Presence

of prognostically insignificant extrahepatic metastatic disease was not considered a contraindication. For RE, <sup>90</sup>yttrium-loaded microspheres (either SIR-Spheres; SIRTEX Medical Europe, Germany or Theraspheres; BTG, Canada) were used. All patients received lobar RE, either of the right or left liver lobe. The applied activity was determined by percentage of tumor involvement of the liver and body surface area.

## Pretherapeutic and Posttherapeutic Imaging Protocol

Imaging studies followed a standardized protocol (Table 1). Whole-body contrast-enhanced <sup>18</sup>F-FDG PET/CT of the neck, thorax, abdomen, and pelvis was performed and included contrast-enhanced imaging in all baseline examinations and in 16 of the 35 patients on early follow-up PET/CT. Liver MRI was performed on a 1.5-T system and included a dynamic contrast-enhanced series as well as T2-weighted and DWI sequences in all cases.

**TABLE 1.** Image Acquisition Protocol for PET/CT and MRI

<b>Table 1A</b>	<b>PET/CT</b>		
Type of scanner	Gemini TF 16, Philips Healthcare, Best, The Netherlands		
PET tracer	<sup>18</sup> F-FDG		
Dose of PET tracer	3 MBq/kg		
Type of contrast agent	Iopromide 300/370 (Ultravist 300/370, Bayer-Schering, Germany)		
Dose of contrast agent	120–148 mL		
	Whole-body low-dose CT	Contrast-enhanced CT (portal venous phase)	PET
Collimation	16 × 1.5 mm	16 × 0.75 mm	n.a.
Pitch	0.812	0.813	n.a.
Rotation time	0.4 s	0.75 s	n.a.
Acquisition matrix	n.a.	n.a.	144 × 144
Field of view	n.a.	n.a.	576 mm
Section thickness	5/1 mm	5/1 mm	4 mm
Effective tube current-time product	30 mAs	200 mAs	n.a.
Tube voltage	120 kV(p)	120 kV(p)	n.a.
Acquisition time per bed position	n.a.	n.a.	1.5 min.
Delay after contrast medium injection	n.a.	70 s	n.a.
<b>Table 1B</b>	<b>MRI</b>		
Type of scanner	1.5-T Achieva, Philips Healthcare, Best, The Netherlands		
Surface coil	Multielement 16-channel coil (Sense Torso XL)		
Type of contrast agent	Gd-DTPA (Magnevist, Bayer-Schering, Leverkusen, Germany)		
Dose of contrast agent	0.1 mmol/kg of body weight		
	Dynamic series	T2-weighted pulse sequence*	Diffusion-weighted imaging
Pulse sequence type	T1-weighted 3D gradient echo	2D turbo spin echo	2D single-shot SE EPI
TR/TE, ms	4.3/1.3	2500/80	1400/63
Orientation	Axial	Axial	Axial
Acquisition matrix	268 × 174	304 × 233	112 × 110
Field of view	330 mm	310 mm	380 mm
Section thickness	8 mm	7 mm	7 mm
Breath compensation	Breath-hold	Respiratory triggering and breath-hold	Respiratory triggering
Sense factor	2	1.4	2
b Values	n.a.	n.a.	0, 50, 800
No. dynamics	1 precontrast, 3 postcontrast with bolus tracking (arterial, portal-venous, equilibrium phase)	n.a.	n.a.

\*Acquired in axial and coronal planes with and without fat saturation.

<sup>18</sup>F-FDG indicates fluorodeoxyglucose; 2D, 2-dimensional; 3D, 3-dimensional; CT, computed tomography; EPI, echo planar imaging; Gd-DTPA, gadolinium-diethylenetriamine penta-acetic acid; MRI, magnetic resonance imaging; n.a., not applicable; PET, positron emission tomography; SE, spin echo.

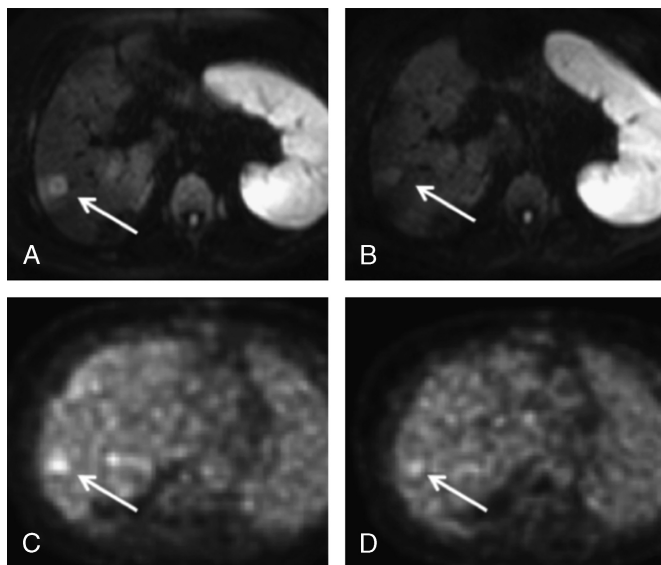


**FIGURE 1.** Assessment of treatment response in a 71-year-old female patient with metastatic colorectal cancer. Upper row (A, B), Diffusion-weighted imaging with b values of 800 s/mm<sup>2</sup> before and 30 days after treatment of the right liver lobe by Y90-RE. Bottom row (C, D), Corresponding SUV maps. Arrows indicate the same lesion on all images. In her case, ADC<sub>min</sub> increased from  $0.55 \times 10^{-3}$  mm<sup>2</sup>/s (A) to  $0.93 \times 10^{-3}$  mm<sup>2</sup>/s (B) and SUV<sub>max</sub> decreased from 5.0 (C) to 3.9 (D). Follow-up confirmed response to treatment.

## Target Lesion Selection and Response Assessment

### Target Lesion Selection

All target lesions were defined on baseline imaging studies in cooperation between an abdominal radiologist and a nuclear medicine specialist who were blinded to the respective outcome of the patients. Target lesions were chosen on the basis of the baseline liver MRI and PET/CT images and selected in accordance with RECIST criteria in that they appeared best measurable and representative of a patient's overall tumor load (Fig. 1). For each patient, at least 3 target lesions with a diameter of at least 1 cm were defined.

### Analysis of SUV and ADC

On a dedicated workstation (Imalytics; Philips Medical Imaging, Best, The Netherlands), the SUV and ADC values were quantified on the registered PET/CT data and on MRI, respectively. Care was taken to include the same target lesions on MRI and PET as well as on baseline and follow-up images. Through manual rendering of each target lesion, volumes of interest were generated. Care was taken to avoid partial-volume averaging through inclusion of adjacent nonmetastatic liver tissue. The maximum standard uptake value (SUV<sub>max</sub>) and minimal apparent diffusion coefficient (ADC<sub>min</sub>) were determined for each lesion. For each patient, the results of the 3 lesions were averaged. Quantitative values were dichotomized to distinguish responders from nonresponders. A positive response to Y90-RE (responder) was defined as a reduction of mean SUV<sub>max</sub> by more than 30%<sup>7,23</sup> or as an increase of mean ADC<sub>min</sub> by more than 30%.

### Analysis of Tumor Size and Contrast Enhancement

Size of target lesions was measured in accordance with RECIST guidelines<sup>3</sup> on both magnetic resonance (MR) and CT images before and after treatment. Contrast enhancement of target lesions on MR and CT images was assessed by 2 radiologists in consensus according to a 5-point scale from 1 (devascularized tumor without visible arterial

or late contrast enhancement) through 5 (strong perfusion with arterial enhancement well beyond that of normal liver).

### Validation of Response Classification

To validate response classification, a conjoint review of all existing information on a given patient, including serological data (eg, tumor marker development) and tumor size changes on long-term follow-up (>12 months or until progression) contrast-enhanced MRI and PET/CT imaging, was used to establish presence or absence of response. Patient outcome, especially with regard to response to liver-directed treatment, was evaluated by an independent consortium that reviewed imaging findings, laboratory values including appropriate tumor marker depending on the type of primary tumor, and patient Eastern Cooperative Oncology Group performance status. A measurable and persistent decrease in size of the target lesions on follow-up imaging over time, with a follow-up of at least 6 months, was taken as evidence of response. Response was also assumed when tumor size remained stable, but a substantial drop of tumor markers occurred, and/or signs of regression such as calcifications or absence of enhancement were seen. On the basis of patient outcome, response classifications made by SUV and DWI changes were categorized as true or false. This was then used to calculate the sensitivity with which the imaging method was able to detect response to treatment, as well as positive and negative predictive values (PPV, NPV) for diagnosing presence or absence of response.

### Statistical Analysis

Continuous variables are expressed as mean values  $\pm$  standard deviation. The Spearman correlation coefficient assessed the degree of monotonic association between ADC<sub>min</sub> and SUV<sub>max</sub>. Changes in SUV<sub>max</sub>, ADC<sub>min</sub>, and tumor size were evaluated using the paired Wilcoxon test. Sensitivity for demonstrating response was compared using the McNemar test. All test results were analyzed in an explorative way; thus, *P* values of *P*  $\leq$  0.05 were regarded as statistically significant. The interpretation of correlation tests followed the guidelines according to Altman.<sup>24</sup> All statistical analyses were conducted using SAS version 9.2 (SAS Institute).

## RESULTS

### Patients and Target Lesions

Thirty-five patients (24 females, 11 males) met the inclusion criteria (Table 2). The primary tumors were colorectal cancer in 20, breast cancer in 13, as well as 1 case each of pharyngeal carcinoma and cancer of unknown primary. Because 3 target lesions were evaluated in each patient (and averaged), a total of 105 target lesions were included in the analysis.

### Radioembolization

A total of 8 of the 35 patients received RE of the left liver lobe with a mean activity of  $0.69 \pm 0.21$  GBq; 27/35 patients underwent treatment of the right liver lobe with a mean activity of  $1.21 \pm 0.40$  GBq. Two patients received RE with glass microspheres; all other patients received resin microspheres.

### Changes in Tumor Size and Contrast Enhancement

Size of target lesions was established on both CT and MR images. No statistically significant changes of tumor size was observed in either CT or MR imaging in the studies before vs. after treatment. As is typical for secondary liver malignancies, the vast majority of metastases was only moderately hypervascular. No significant change of contrast enhancement patterns was observed in the contrast-enhanced studies before versus that after treatment, either for dynamic contrast-enhanced MRI or for contrast-enhanced CT imaging (Table 3).

**TABLE 2.** Characteristics of the Study Cohort

Study Population (n = 35)			
Demographic details	Age	y	60 ± 10
	Sex	f/m	24/11
Type of Primary	Breast cancer	n	13
	Colorectal cancer	n	20
	Pharyngeal cancer	n	1
	CUP	n	1
Oncologic situation	No. patients with additional extrahepatic metastases	n	21
	No. patients who had received prior systemic therapy	n	35
Timing of imaging and RE	Time since initial tumor diagnosis to RE	mo	47 ± 57
	Average time between baseline MRI and RE	d	21 ± 7
	Time between baseline PET/CT and RE	d	22 ± 7
	Patients in whom baseline DWI and PET/CT were performed on the same day	n	15
	Average time between RE and follow-up MRI and follow-up PET/CT	d	35 ± 5
Patients in whom follow-up MRI and PET/CT were performed on the same day	n	32	

CT indicates computed tomography; CUP, cancer of unknown primary; MRI, magnetic resonance imaging; PET, positron emission tomography; RE, radioembolization.

### Changes in SUV

The average SUVmax change after RE was  $-2.5 \pm 3.9$  ( $-23.6 \pm 31.4\%$ ) ( $P < 0.0001$ ) (Table 3). A total of 17 (49%) of the 35 patients showed an overall SUVmax decrease by more than 30% and were therefore classified as “responders.” Four patients (4/35; 11%) with metastatic breast cancer were classified as “not assessable” with PET because the respective metastases were PET-negative, that is, did not exhibit a perceptibly or measurably increased SUV compared with the surrounding normal liver tissue. The remaining 14 (40%) of the 35 were classified as “nonresponders.”

In the SUV-responder group, the average SUVmax change was  $-5.2 \pm 3.9$  ( $-50.0\% \pm 12.4\%$ ).

In the SUV-nonresponder group, the average SUVmax change was  $0.0 \pm 1.6$  ( $0.8\% \pm 23.4\%$ ).

### Changes in ADC

The average ADCmin change after RE was  $0.6 \pm 0.3 \times 10^{-3}$   $\text{mm}^2/\text{s}$  ( $57.7\% \pm 76.3\%$ ) ( $P < 0.0001$ ) (Table 3). A total of 23 (66%) of the 35 patients showed an increase of ADCmin by higher than 30% and were therefore categorized as responders to RE. The remaining 12 (34%) of the 35 were classified as nonresponders. All metastases

had a strong correlate on baseline DWI; accordingly, none of the patients was categorized as not assessable.

In the ADC-responder group, the average ADCmin increase was  $0.4 \pm 0.2 \times 10^{-3}$   $\text{mm}^2/\text{s}$  ( $93.3\% \pm 70.1\%$ ).

In the ADC-nonresponder group, the average ADCmin decrease was  $-0.1 \pm 0.1 \times 10^{-3}$   $\text{mm}^2/\text{s}$  ( $-10.4\% \pm 21.5\%$ ).

### Correlation Between ADC and SUV Changes

For the entire group of 35 patients, pretherapeutic versus post-therapeutic changes of ADCmin and changes of SUVmax correlated moderately ( $r = -0.43$ ). When the 4 PET-negative patients were excluded from the analysis, a moderate correlation was found between changes in ADCmin and changes in SUVmax ( $r = -0.53$ ) (Fig. 2).

### Response Classification Based on ADC and SUV Changes

Concordant response classification was observed in 25 of the 35 patients, with 15 (60%) of the 25 patients concordantly classified as responders and 10 (40%) of the 25 patients concordantly classified as nonresponders.

Discordant response classification was observed in 6 of the 35 patients. In 4 of these 6 patients, ADC-based analysis suggested

**TABLE 3.** Changes of Tumor Size, Arterial Perfusion, ADCmin, and SUVmax Before Versus After Y90-RE

Parameter	Absolute Difference Compared With Baseline Value ± SD	Relative Change Compared With Baseline Value ± SD	P
RECIST size measurement based on CT images	$-0.9 \pm 4.8$ mm	$-3.9\% \pm 18.3\%$	>0.05
RECIST size measurement based on MR images	$-0.7 \pm 4.8$ mm	$-4.1\% \pm 16.9\%$	>0.05
Enhancement on CT*	$0.4 \pm 1.2$	n.a.	>0.05
Enhancement on DCE MRI*	$0.3 \pm 1.1$	n.a.	>0.05
SUVmax in PET	$-2.5 \pm 3.9$	$-23.6\% \pm 31.4\%$	<0.0001
ADCmin in DWI-MRI	$0.6 \pm 0.3 \times 10^{-3}$ $\text{mm}^2/\text{s}$	$57.7\% \pm 76.3\%$	<0.0001

\*Categorical values from 1 (absent enhancement) to 5 (strong arterial contrast enhancement).

ADCmin indicates minimal apparent diffusion coefficient; CT, computed tomography; DCE MRI, dynamic contrast-enhanced magnetic resonance imaging; DWI-MRI, diffusion-weighted magnetic resonance imaging; MR, magnetic resonance; n.a., not applicable; RECIST, Response Evaluation Criteria in Solid Tumors; SUVmax, maximum standardized uptake value; Y90-RE, Y90-radioembolization.

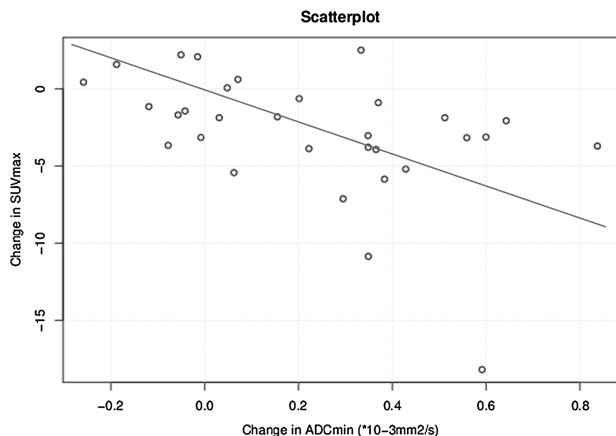


**FIGURE 2.** Correlation between ADCmin and SUVmax changes before and after RE in all assessable patients (n = 31) ( $r = -0.53$ ).

presence, whereas the SUV-based analysis suggested absence of response. In the remaining 4 of the 35 patients with PET-negative metastases, no DWI/PET correlation of response could be established.

**Results on Follow-Up**

On the basis of clinical and imaging follow-up, 23 (66%) of the 35 patients responded to the Y90-treatment, whereas 12 (34%) of the 35 did not. The follow-up confirmed the ADC-based response classifications in 5 of the 6 patients with divergent response classification (Table 4).

This yields a PPV (prediction of presence of response) of 22 (96%) of 23 for DWI-MRI and 15 (88%) of 17 for PET. The NPV (prediction of absence of response) was 11 (92%) of 12 for MRI and 10 (56%) of 18 for PET. The sensitivity for demonstrating response was significantly higher for MRI (22/23; 96%) than for PET (15/23; 65%) ( $P < 0.02$ ; Table 5).

**DISCUSSION**

In this cohort of 35 patients with liver metastases caused by common solid cancers, we found a moderate inverse correlation between ADCmin and SUVmax changes after the Y90-RE ( $r = -0.53$ ). Both functional imaging methods helped detect response to treatment early, that is, before any statistically significant changes of tumor size or those

**TABLE 4.** Comparison of Response Assessment With Patient Outcome

		Validation: Responder	Validation: Nonresponder	Sum
Response assessment based on PET	PET positive (responder)	15	2	17
	PET negative (nonresponder)	4	10	14
	PET inconclusive (not assessable)	4	0	4
	Sum	23	12	35
Response assessment based on DWI	DWI positive (responder)	22	1	23
	DWI negative (nonresponder)	1	11	12
	DWI inconclusive (not assessable)	0	0	0
	Sum	23	12	35

DWI indicates diffusion-weighted imaging; PET, positron emission tomography.

**TABLE 5.** Sensitivity and Positive and Negative Predictive Values for Predicting Response

	Sensitivity (%)	PPV (%)	NPV (%)
Response assessment based on PET	15/23 (65%) [45%–81%]	15/17 (88%) [64%–99%]	10/18 (56%) [31%–78%]
Response assessment based on DWI	22/23 (96%) [78%–100%]	22/23 (96%) [78%–100%]	11/12 (92%) [62%–100%]

Numbers in square brackets represent 95% confidence intervals.

DWI indicates diffusion-weighted imaging; NPV, negative predictive value; PET, positron emission tomography; positive predictive value.

of contrast enhancement were observable on contrast-enhanced MRI or CT imaging. However, we found that changes of DWI-derived parameters (ADCmin) were more accurate in predicting response than that of PET-derived parameters (SUVmax), both in terms of demonstrating response as well as in terms of suggesting absence of response. This, together with the fact that, in 11% of patients (4/35), response assessment based on PET was a priori impossible because metastases were PET-negative on baseline PET, led to the fact that DWI proved to be significantly more sensitive than PET: DWI helped predict response with a sensitivity and PPV of 96%, compared with 65% and 88%, respectively, for PET.

Positron emission tomography/computed tomography is currently considered to represent the standard of reference for assessing early response to nonsurgical, systemic, or regional treatment of liver metastases.<sup>7,25,26</sup> There is a growing body of evidence to suggest that DWI can provide similar, although physiologically more or less unrelated, diagnostic information.<sup>18–22</sup> Probably owing to the high cellularity, the high interstitial pressure, and/or the irregular internal architecture, diffusion of free water is restricted in cancerous tissue, yielding low ADC values.<sup>27</sup> This has been exploited for oncologic applications in several ways: (1) to improve detection of cancer, for example, of liver metastases in hepatic MRI<sup>28,29</sup> or of lymph node metastases in whole-body MRI<sup>30,31</sup>; (2) to provide an imaging biomarker for tumor cellularity and, hence, biologic importance of, for example, prostate cancer<sup>32</sup>; (3) to help predict response of, for example, rectal cancer to regional or systemic treatment<sup>18</sup>; and (4) to monitor response to neoadjuvant chemotherapy or radiochemotherapy of primary breast, gastroesophageal, and rectal cancers<sup>14–20</sup> and also, more recently, to assess response to local treatment of hepatocellular cancer.<sup>33</sup>

However, there is little evidence on the use of DWI to monitor treatment response of liver metastases. Moreover, beyond mere correlation studies, the actual diagnostic accuracy (ie, sensitivity and predictive values) with which DWI or PET detects early response to treatment has not yet been established. This, however, is important if functional imaging is to be used to guide treatment decisions in clinical interventional oncology.

Transarterial radioembolization by <sup>90</sup>yttrium (Y90-RE) is recognized as a salvage treatment option mainly for patients with hepatocellular cancer<sup>31</sup> but is increasingly used also in patients with secondary liver cancer due to colorectal, neuroendocrine, and breast cancer who exhibit a hepatic tumor load that appears prognostically relevant and does not respond to appropriate systemic treatment.<sup>34</sup>

Y90-radioembolization is a palliative regional treatment option that is well suited to document the utility of early response assessment. Patients with hepatic metastases who are candidates for Y90-RE usually have advanced tumor stages with involvement of both liver lobes. Per current guidelines, these patients have usually undergone several cycles of systemic chemotherapy before Y90-RE is at all considered as a

treatment option. Many systemic chemotherapy regimens are potentially hepatotoxic and may impair the functional reserve of the liver, a situation that may not be readily obvious from regular liver function tests. The concept of all types of transarterial treatment strategies implies that the active agent (eg, Y90 particles) should lodge preferentially in the vascular network that is built around malignant liver tissue and that is supplied mainly by the hepatic artery.<sup>35</sup> Whereas a high degree of arterialization is reliably present in primary liver (hepatocellular) cancer, this supply is more variable in patients with secondary liver tumors.<sup>36–38</sup> In addition, antiangiogenic agents (eg, bevacizumab), an integral part of many contemporary systemic treatment regimens for liver metastases, may modify the type and degree of effective arterial supply and, accordingly, the gradient between metastatic and normal liver arterialization.<sup>39,40</sup> Accordingly, although Y90-RE has been shown to be a safe and effective treatment for patients with secondary liver cancer, patient selection is challenging because the final dose distribution is difficult to anticipate.<sup>41,42</sup>

To reduce the risk for Y90-RE–induced liver function impairment, Y90-RE for diffuse liver metastases is provided in a lobar fashion.<sup>43</sup> This means that patients usually undergo treatment of one half of the liver at a time, whereas the second treatment session for the other half is provided 4 to 8 weeks apart, depending on the clinical tolerability and liver function after the first treatment session.

So far, guidelines do not require or support the use of imaging to assess response in between lobar treatment sessions.<sup>44</sup> This is because it has been shown that early response to Y90-RE is difficult to detect; tumor size changes may take a couple of months to be observable on state-of-the-art cross-sectional imaging methods. However, to avoid additional and possibly futile strain to the patient, it would be highly desirable to know about the therapeutic efficacy of Y90-RE in the individual patient before treatment of the second half of the liver is initiated. In patients with secondary liver cancer, this would also be important for further patient management, for example, initiation of further systemic chemotherapy.

In our study, PET/CT and DWI-MRI were obtained early after the first treatment session, that is, within 35 days after lobar Y90-RE, to investigate the accuracy with which DWI-MRI can predict response to treatment compared with FDG-PET. Our results suggest that this accuracy is not only comparable but indeed also significantly higher than that achieved by PET imaging. The 2 methods yielded concordant results with regard to response classification in 25 (81%) of 31 patients who were PET-positive. In 5 of 6 patients with diverging classification of response, clinical and imaging follow-up confirmed the response assessment provided by DWI-MRI. In another 4 patients, each with metastatic breast cancer, PET was not useful for response assessment because the metastases were PET-negative. This translated into a significantly higher sensitivity of DWI-MRI versus PET ( $P < 0.02$ ) for demonstrating early response in patients undergoing Y90-RE procedures.

Our results suggest that, in patients undergoing lobar Y90 therapy for secondary liver tumors, it may be useful to perform DWI after the first treatment session. Failure to respond to lobar RE, as diagnosed by the absence of an increase of ADC<sub>min</sub>, may then be used to spare the patient from an unnecessary (ie, ineffective) additional treatment session of the contralateral lobe. This will be important especially in patients with borderline liver function. Although such close monitoring of treatment response will not be needed in the majority of patients undergoing systemic chemotherapy for liver metastases, further research on the use of DWI-MRI for assessing response not only to local but also to systemic treatment seems justified.

Besides, our results underscore once more the utility of Y90-RE for palliative treatment of patients with therapy-refractory liver metastases. Of the 35 patients with prognostically relevant hepatic metastases who had been progressive under state-of-the-art systemic chemotherapy and targeted therapy, 23 (66%) did respond to the treatment.

The main limitation of our study is the small number of patients; further prospective studies are needed to validate our results in a larger group of patients. Moreover, all patients had advanced stages of liver metastases and had undergone a number of different systemic therapy cycles; this may confound the results of response assessment. However, our patients underwent systemic treatment in accordance with current international guidelines on the basis of decisions made in multidisciplinary tumor conferences in each individual patient case; accordingly, it is likely that the confounding effects of prior systemic chemotherapy will be representative for all patients with liver metastases treated with Y90-RE.

We conclude that DWI-MRI appears superior to PET/CT for early assessment of treatment response in patients with hepatic metastases of common solid tumors (colorectal, breast). Diffusion-weighted magnetic resonance imaging accurately predicts response before changes of tumor size or contrast enhancement are observable on contemporary cross-sectional imaging such as contrast-enhanced MRI or CT. It may therefore be useful to guide treatment decisions in patients undergoing lobar Y90-RE.

## REFERENCES

- Vente MA, Wondergem M, van der Tweel I, et al. Yttrium-90 microsphere radioembolization for the treatment of liver malignancies: a structured meta-analysis. *Eur Radiol*. 2009;19:951–959.
- Kennedy A, Salem R. Radioembolization (yttrium-90 microspheres) for primary and metastatic hepatic malignancies. *Cancer J*. 2010;16:163–175.
- Eisenhauer EA, Therasse P, Bogaerts J, et al. New response evaluation criteria in solid tumors: revised RECIST guideline (version 1.1). *Eur J Cancer*. 2009;45:228–247.
- Bester L, Hobbins PG, Wang SC, et al. Imaging characteristics following 90yttrium microsphere treatment for unresectable liver cancer. *J Med Imaging Radiat Oncol*. 2011;55:111–118.
- Bienert M, McCook B, Carr BI, et al. 90Y microsphere treatment of unresectable liver metastases: changes in 18 F-FDG uptake and tumor size on PET/CT. *Eur J Nucl Med Mol Imaging*. 2005;32:778–787.
- Szyszko T, Al-Nahhas A, Canelo R, et al. Assessment of response to treatment of unresectable liver tumors with 90Y microspheres: value of FDG PET versus computed tomography. *Nucl Med Commun*. 2007;28:15–20.
- Haug A, Donfack BPT, Trumm C, et al. 18 F-FDG PET/CT predicts survival after radioembolization of hepatic metastases from breast cancer. *J Nucl Med*. 2012;53:371–377.
- Schmidt H, Brendle C, Schraml C, et al. Correlation of simultaneously acquired diffusion-weighted imaging and 2-deoxy-[18 F] fluoro-2-D-glucose positron emission tomography of pulmonary lesions in a dedicated whole-body magnetic resonance/positron emission tomography system. *Invest Radiol*. 2013;48:247–255.
- Hamstra DA, Rehemtulla A, Ross BD. Diffusion magnetic resonance imaging: a biomarker for treatment response in oncology. *J Clin Oncol*. 2007;25:4104–4109.
- Chenevert TL, Meyer CR, Moffat BA, et al. Diffusion MRI: a new strategy for assessment of cancer therapeutic efficacy. *Mol Imaging*. 2002;1:336–343.
- Heijmen L, Ter Voert EE, Nagtegaal ID, et al. Diffusion-weighted MR imaging in liver metastases of colorectal cancer: reproducibility and biological validation. *Eur Radiol*. 2013;23:748–756.
- Genovesi D, Filippone A, Ausili Cèfaro G, et al. Diffusion-weighted magnetic resonance for prediction of response after neoadjuvant chemoradiation therapy for locally advanced rectal cancer: preliminary results of a monoinstitutional prospective study. *Eur J Surg Oncol*. 2013;39:1071–1078.
- Lin C, Itti E, Luciani A, et al. Whole-body diffusion-weighted imaging with apparent diffusion coefficient mapping for treatment response assessment in patients with diffuse large B-cell lymphoma: pilot study. *Invest Radiol*. 2011;46:341–349.
- Giganti F, De Cobelli F, Canevari C, et al. Response to chemotherapy in gastric adenocarcinoma with diffusion-weighted MRI and 18 F-FDG-PET/CT: correlation of apparent diffusion coefficient and partial volume corrected standardized uptake value with histological tumor regression grade. *J Magn Reson Imaging*. 2014;40:1147–1157.
- Gong NJ, Wong CS, Chu Y, et al. Treatment response monitoring in patients with gastrointestinal stromal tumor using diffusion-weighted imaging: preliminary results in comparison with positron emission tomography/computed tomography. *NMR Biomed*. 2013;26:185–192.

16. Weber MA, Bender K, von Gall CC, et al. Assessment of diffusion-weighted MRI and 18 F-fluoro-deoxyglucose PET/CT in monitoring early response to neoadjuvant chemotherapy in adenocarcinoma of the esophagogastric junction. *J Gastrointest Liver Dis.* 2013;22:45–52.
17. Schmidt S, Dunet V, Koehli M, et al. Diffusion-weighted magnetic resonance imaging in metastatic gastrointestinal stromal tumor (GIST): a pilot study on the assessment of treatment response in comparison with 18 F-FDG PET/CT. *Acta Radiol.* 2013;52:837–842.
18. Ippolito D, Monguzzi L, Guerra L, et al. Response to neoadjuvant therapy in locally advanced rectal cancer: assessment with diffusion-weighted MR imaging and 18FDG PET/CT. *Abdom Imaging.* 2012;37:1032–1040.
19. Ohno Y, Koyama H, Yoshikawa T, et al. Diffusion-weighted MRI versus 18 F-FDG PET/CT: performance as predictors of tumor treatment response and patient survival in patients with non-small cell lung cancer receiving chemoradiotherapy. *AJR Am J Roentgenol.* 2012;198:75–82.
20. Park SH, Moon WK, Cho N, et al. Comparison of diffusion-weighted MR imaging and FDG PET/CT to predict pathological complete response to neoadjuvant chemotherapy in patients with breast cancer. *Eur Radiol.* 2012;22:18–25.
21. Dudeck O, Zeile M, Wybranski C, et al. Early prediction of anticancer effects with diffusion-weighted MR imaging in patients with colorectal liver metastases following selective internal radiotherapy. *Eur Radiol.* 2010;20:2699–2706.
22. Li Z, Bonekamp S, Halappa VG, et al. Islet cell liver metastases: assessment of volumetric early response with functional MR imaging after transarterial chemoembolization. *Radiology.* 2012;264:97–109.
23. Wahl RL, Jacene H, Kasamon Y, et al. From RECIST to PERCIST: evolving considerations for PET response criteria in solid tumors. *J Nucl Med.* 2009;50 (suppl 1):122S–150S.
24. Altman DG. *Practical Statistics for Medical Research.* London, England: Chapman & Hall/CRC; 1990.
25. Findlay M, Young H, Cunningham D, et al. Noninvasive monitoring of tumor metabolism using fluorodeoxyglucose and positron emission tomography in colorectal cancer liver metastases: correlation with tumor response to fluorouracil. *J Clin Oncol.* 1996;14:700–708.
26. Lastoria S, Piccirillo MC, Caracò C, et al. Early PET/CT scan is more effective than RECIST in predicting outcome of patients with liver metastases from colorectal cancer treated with preoperative chemotherapy plus bevacizumab. *J Nucl Med.* 2013;54:2062–2069.
27. Miller FH, Hammond N, Siddiqi AJ, et al. Utility of diffusion-weighted MRI in distinguishing benign and malignant hepatic lesions. *J Magn Reson Imaging.* 2010;32:138–147.
28. Frankel TL, Gian RK, Jarnagin WR. Preoperative imaging for hepatic resection of colorectal cancer metastasis. *J Gastrointest Oncol.* 2012;3:11–18.
29. Yu JS, Chung JJ, Kim JH, et al. Detection of small intrahepatic metastases of hepatocellular carcinomas using diffusion-weighted imaging: comparison with conventional dynamic MRI. *Magn Reson Imaging.* 2011;29:985–992.
30. Gu J, Chan T, Zhang J, et al. Whole-body diffusion-weighted imaging: the added value to whole-body MRI at initial diagnosis of lymphoma. *AJR Am J Roentgenol.* 2011;197:384–391.
31. Eiber M, Holzapfel K, Ganter C, et al. Whole-body MRI including diffusion-weighted imaging (DWI) for patients with recurring prostate cancer: technical feasibility and assessment of lesion conspicuity in DWI. *J Magn Reson Imaging.* 2011;33:1160–1170.
32. Panebianco V, Sciarra A, Marcantonio A, et al. Conventional imaging and multiparametric magnetic resonance (MRI, MRS, DWI, MRP) in the diagnosis of prostate cancer. *Q J Nucl Med Mol Imaging.* 2012;56:331–342.
33. Kokabi N, Camacho JC, Xing M, et al. Apparent diffusion coefficient quantification as an early imaging biomarker of response and predictor of survival following yttrium-90 radioembolization for unresectable infiltrative hepatocellular carcinoma with portal vein thrombosis. *Abdom Imaging.* 2014;39:969–978.
34. Salem R, Mazzaferro V, Sangro B. Yttrium 90 radioembolization for the treatment of hepatocellular carcinoma: biological lessons, current challenges, and clinical perspectives. *Hepatology.* 2013;58:2188–2197.
35. Bester L, Meteling B, Boshell D, et al. Transarterial chemoembolisation and radioembolisation for the treatment of primary liver cancer and secondary liver cancer: a review of the literature. *J Med Imaging Radiat Oncol.* 2014;58:341–352.
36. Lewandowski RJ, Geschwind JF, Liapi E, et al. Transcatheter intraarterial therapies: rationale and overview. *Radiology.* 2011;259:641–657.
37. Yang ZF, Poon RT. Vascular changes in hepatocellular carcinoma. *Anat Rec (Hoboken).* 2008;291:721–734.
38. Muto J, Shirabe K, Sugimachi K, et al. Review of angiogenesis in hepatocellular carcinoma. *Hepatol Res.* 2015;45:1–9.
39. Van de Wiele C, Maes A, Brugman E, et al. SIRT of liver metastases: physiological and pathophysiological considerations. *Eur J Nucl Med Mol Imaging.* 2012;39:1646–1655.
40. Loupakis F, Schirripa M, Caparello C, et al. Histopathologic evaluation of liver metastases from colorectal cancer in patients treated with FOLFOXIRI plus bevacizumab. *Br J Cancer.* 2013;108:2549–2556.
41. Ulrich G, Dudeck O, Furth C, et al. Predictive value of intratumoral <sup>99m</sup>Tc-macroaggregated albumin uptake in patients with colorectal liver metastases scheduled for radioembolization with <sup>90</sup>Y-microspheres. *J Nucl Med.* 2013;54:516–522.
42. Lau WY, Kennedy AS, Kim YH, et al. Patient selection and activity planning guide for selective internal radiotherapy with yttrium-90 resin microspheres. *Int J Radiat Oncol Biol Phys.* 2012;82:401–407.
43. Seidensticker R, Seidensticker M, Damm R, et al. Hepatic toxicity after radioembolization of the liver using (90)Y-microspheres: sequential lobar versus whole liver approach. *Cardiovasc Intervent Radiol.* 2012;35:1109–1118.
44. Kennedy A, Nag S, Salem R, et al. Recommendations for radioembolization of hepatic malignancies using yttrium-90 microsphere brachytherapy: a consensus panel report from the radioembolization brachytherapy oncology consortium. *Int J Radiat Oncol Biol Phys.* 2007;68:13–23.